IEEE Access
Multidisciplinary | Rapid Review | Open Access Journal

Received September 29, 2021, accepted October 24, 2021, date of publication November 2, 2021,
date of current version November 11, 2021.

Digital Object Identifier 10.1109/ACCESS.2021.3124923

Hybrid Precoding Aided Fast Frequency-Hopping for Millimeter-Wave Communication

ABBAS AHMED[1], QASIM ZEESHAN AHMED[2], (Member, IEEE), AHMAD ALMOGREN[3], (Senior Member, IEEE), SYED KAMRAN HAIDER[1], AND ATEEQ UR REHMAN[4]

[1]Beaconhouse International College, Islamabad 44000, Pakistan
[2]Department of Electronics and Electrical Engineering, University of Huddersfield, Huddersfield HD1 3DH, U.K.
[3]Department of Computer Science, College of Computer and Information Sciences, King Saud University, Riyadh 11633, Saudi Arabia
[4]Department of Electrical Engineering, Government College University, Lahore 54000, Pakistan

Corresponding authors: Abbas Ahmed (abbas.ahmed@bic.edu.pk) and Ateeq Ur Rehman (ateeq.rehman@gcu.edu.pk)

This work was supported by King Saud University, Riyadh, Saudi Arabia, through researchers supporting project number RSP-2021/184.

ABSTRACT The deployment of the Millimeter-Wave (mm-Wave) band in 5G and beyond wireless communications networks is one of the emerging fields owing to its potential of providing extensive bandwidth. Frequency Hopping (FH) has a high potential for use in wireless networks due to its key advantages of spreading the interference over wide bandwidth and of providing diversity gain in counteracting frequency-selective fading. Furthermore, Fast Frequency Hopping (FFH) intrinsically amalgamated with directional Beamforming (BF) may overcome the impairments because of the path-loss of mm-Wave communications. Thus, we propose FFH assisted base-band precoding aided BF for mitigating the mm-wave channel impairments imposed by both fading as well as path loss, whilst relying on a minimal range of radio frequency chains. The mathematical analysis and simulation results demonstrate that hybrid precoded FFH is indeed a promising high-capacity technique of attaining both time- and frequency-domain diversity gains for the mm-Wave communications.

INDEX TERMS mm-Wave, frequency hopping, 5G, wireless network.

I. INTRODUCTION

The rapid proliferation of mobile devices coupled with increased usage of high bandwidth multimedia application underpins the demand for supporting increased throughput in wireless communication networks [1]–[4]. The recent report of the International Telecommunications Union (ITU) reveals that a minimum peak-rate of 20 Gbps and 10 Gbps for the DownLink (DL) and the UpLink (UL) is required accordingly [5]. The limited spectral resources, available in the lower-part of the current microwave band, fail to meet this ambitious data rate requirement [6]–[9]. Nevertheless, high frequencies transmissions can support substantially higher bandwidth and are currently under utilized [10]. Therefore, the millimeter-wave (mm-Wave) band appears to be a potential solution. It has hence attracted substantial research interests due to benefit of wide bandwidth available [11], [12]. However, the key challenge is that mm-Wave frequencies are severely affected both by a high path loss and by a frequency-selective as well as time-selective fading [13]–[15].

The impediment of severe path loss may be mitigated by employing a highly directional array aided Beam Forming (BF) schemes [16]–[18]. However, as these BF schemes require accurate channel knowledge which is difficult to acquire due to operation over large antenna arrays, gigasample mixed signal devices or wider bandwidths, therefore, new and low complexity signal processing techniques are required [10], [17], [19]. Channel estimation approach has been adopted for mm-Wave systems in [18], [20], [21] and references within. While to avoid gigasample mixed signal devices have been adopted in [3], [22], [23], and references within. However, in this manuscript we conceive a very unique methodology for hybrid digital to analog (DA) precoders by employing Fast Frequency Hopping (FFH) aided BF schemes.

The associate editor coordinating the review of this manuscript and approving it for publication was Wenjie Feng.

Frequency diversity schemes rely on generating multiple frequencies to address these prevalent challenges for transmitting the intended data streams [24], [25]. Therefore, they are capable of mitigating both the fading as well as the interference because the extended periods of deep co-channel fading or high interference, are avoided by hopping to an independently fading and/or interfered frequency [24], [26], [27]. Indeed, when considering FFH systems, during the transmission of a specific data symbol multiple hops maybe traversed [24]. Furthermore, FFH models are also capable of attaining improved gains as a benefit of randomizing bursty errors [24], [28]–[30]. Additionally, FFH models are capable of supporting a huge range of users [31]–[33]. In some of the FFH systems the identical symbols are repeated during several hops, which are associated with a different frequency and a different time slot. The various replicas of the signal are more likely to be subjected to independent fading conditions, especially if the channel fading is fast and can be considered uncorrelated from symbol to symbol. This makes it highly likely that one of the hops, experiences reduced fading [24], [29]. Moreover, the signals received from different hops can be combined for reducing the channel effect significantly at the receiver [24] to reduce the impact of prorogation impairments at the receiver. In other words, diversity combining can improve Signal-to-Interference-plus-Noise-Ratio (SINR) at the receiver side [34]–[38]. One of the earliest notable contributions on FFH diversity combining was made by Lee *et al.* [34]–[38], which was followed by Wang and Jiang [39]. As a further development Teh *et al.* [40] have investigated self-combining based Binary Frequency Shift Keying (BFSK) receivers in Rician fading environments.

Directional BF may be used for mitigating the propagation losses in mm-Wave systems [41], [42], which have substantial bandwidth reserves. However, numerous antennas have to be adopted for achieving a high BF gain by relying on $\lambda/2$ spacing between the antennas, where λ is the wave length [8], [43], [44]. Fortunately, the wavelength is as short as 0.5 cm at 60 GHz, hence numerous 0.25 cm- spaced antennas may be accommodated even by a shirt-pocket-sized handset. However, if a fully digital transmit precoder scheme is adopted in mm-Wave systems, the RF chains will consume excessive power and the hardware complexity will also increase dramatically [17], [45]. By contrast, analog precoders are less complex than digital precoders. Hence, the concept of hybrid BF, where digital processing was ingeniously combined with analog BF [6], [17], [46]–[48]. Hence, a hybrid Digital-to-Analog (D-to-A) precoding model which incorporated with a range of antennas and a small range of RF chains constitutes a compelling technique of balancing the power consumption, the implementation complexity and the performance of these systems. In hybrid systems, analog BF is implemented by the analog phase-shifters with the RF stage, after the digitally precoded signal is forwarded to the transmitted antennas. At the RF end, the RF signals are first phase-shifted and they are processed by the digital combiner in the base-band system.

Currently, in mm-Wave technology two types of methodologies are opted for the hybrid (D-to-A) precoding. Namely first is referred to as Full-Antenna Array Structure (FAAS) and while other a Sub-Antenna Array Structure (SAAS). In the FAAS model, all the transmit antennas are coupled with dedicated RF chains. In this approach the FAAS achieves full analog BF gain, as in this case the number of antennas is greater than the number of RF chains whereas in SAAS, the computational complexity is compacted at the cost of reduced BF gains [23], [49]. It may be anticipated that the later releases of the 5G cellular network will have a mm-Wave band mode [50], [51]. The 4G UL system depends on Single-Carrier-Frequency-Division Multiple-Access (SC-FDMA) [52], which may also find its way into Next Generation (NG) systems. It is also eminently suitable for FH [14], [24].

The Frequency Division Duplex (FDD) models, the DL is calculated at the receiver, then is quantized and feed back to the Transmit Precoder (TPC), which in turn exploits the knowledge of the Channel Impulse Response (CIR) for pre-compensating its effect. More explicitly, based on its CIR estimates, the best TPC matrix is selected from the code-book and feeds back its index to the transmitter. This procedure is often termed as Limited-Feedback Design (LFD). In this context, Song *et.al* designed a code-book for mm-Wave systems utilizing the Orthogonal Matching Pursuit (OMP) technique [53], [54]. A finite modulation alphabet is was designed by Rajashekar and Hanzo [55], which relies on a vector quantization based formulation. Alkhateeb *et-al* [17] designed a code-book for mm-Wave systems using RF features. Furthermore, Clerckx *et-al* [56] introduced the performance analysis of the code-book design, which works according to the code-book entries. In the light of the above discussion, we conceived a low-complexity hybrid beam forming code-book design. Against this background our novel contribution are as under:

- We propose a novel implementation of FFH system in mm-Wave channel by using linear combination techniques. We also compare two linear combination techniques to see which scheme works better in mm-Wave channel.
- We propose FFH aided digital BF assisted with Discrete Fourier Transform (DFT) supported analog RF BF for a limited-feedback assisted mm-Wave system.
- Lastly, we analyse the outage capacity of the resultant system in mm-Wave channels.

Our system model is illustrated in Section II. In Section III, we describe the mm-Wave channel, while in Section V-A, we portray the DFT aided code-book model invoked for analog RF BF. In Section VII, we analyse simulation results followed by conclusions in section VIII. Before proceeding to our system model, Table illustrates symbols used in this paper.

NOMENCLATURE

λ	wave length.
$\oplus$	addition-modulus.
AoA	Angle of Arrival.
AoD	Angle of Departure.
BF	Beamforming.
BFSK	Binary Frequency Shift Keying.
BPSK	Binary Phase Shift Keying.
BS	Base Station.
CIR	Channel Impulse Response.
DFT	Discrete Fourier Transform.
DL	Downlink.
D to A	Digital-to-Analog.
FAAS	Full-Antenna Array Structure.
FDD	Frequency Division Duplex.
FFH	Fast Frequency Hopping.
FFT	Fast Fourier Transform.
FH	Frequency Hopping.
f_c	carrier frequency.
$f_l^{(k)}$	frequency tone.
GF	Galois Field.
H	Statistical Channel Model.
IFFT	Inverse Fast Fourier Transform.
ITU	International Tele- -communications Union.
NG	Next Generation.
mm-Wave	millimeter-wave.
MFSK	Multiple Frequency-Shift Keying.
MS	Mobile Station.
MUB	Mutually Unbiased Bases.
LFD	Limited-Feedback Design.
L	Diversity order.
P_s	Power Signal.
$p(t)$	The normalised pulse waveform.
PN	Pseudorandom-Noise.
P_e	Probability of Error.
OMP	Orthogonal Matching Pursuit.
RF	Radio Frequency.
R_b	bit rate.
SAD	Sub-Array Design.
SAAS	Sub-Antenna Array Structure.
SC-FDMA	Single-Carrier-Frequency -Division-Multiple-Access.
SFH	Slow Frequency Hoping.
SINR	Signal-to-Interference-plus-Noise-Ratio.
SNR	Signal to Noise Ratio.
S/P	Serial-to-Parallel.
TPC	Transmit Precoder.
T_b	Binary Input period.
T_h	Dwell Time, Time-slots Duration.
T_s	Symbol Duration.
U	Sub-Stream.
UL	UpLink.
ULA	Uniform Linear Array.
X_k	Symbol generated by k^{th} user.

II. SYSTEM MODEL

The architecture of the system proposed is depicted in Fig. 1, which comprises of three parts: the transmitter, the mm-Wave channel and the receiver in detailed in the succeeding sub-sections.

A. TRANSMITTER MODEL

A basic architecture of FFH-Multiple Frequency-Shift Keying (MFSK) transmitter is shown in Fig. 2. It is anticipated that all communication from mobile User Equipment (UE) is scheduled by the BS on the link which employs FFH-MFSK transmission [24], [57]–[59]. It is reflected from Fig. 2 that the enormous data rates consists of sub-stream U, where the operation of MFSK and FFH are carried out at each sub-streams to transmit the data to the receiver. From Fig. 2, the period of the binary input is T_b having a rate R_b of the first Serial-to-Parallel (S/P) converter to transfer U parallel sub-streams. In the process of symbol-duration T_s, every sub-stream generates $b = \log_2(M)$ bits which form a MFSK symbol [22], [34], [60]. In the attempt to execute the FFH, the duration of the symbol is denoted as $T_s = UbT_b$. Additionally, the T_s is divided into L chips or hops where T_h can be quantified as $T_h = T_s/L$, and represents the number of time-slots duration. In FFH model illustrated in Fig. 2, where the system bandwidth is shared by the total number of K users. The k^{th} user address is randomly and uniquely assigned by utilizing the Pseudorandom-Noise (PN) code and is represented as

$$\boldsymbol{a}_k = [a_k(0), a_k(1), \cdots, a_k(L-1)], \tag{1}$$

where $l = 0, 1, \cdots, L-1$, $a_k(l) \in GF(M)$ and $GF(M)$ represents the Galois Field with M number of elements. X_k is the first designated symbol and

$$\boldsymbol{y}_k = [y_k(0), y_k(1), \cdots, y_k(L-1)] = X_k \cdot \mathbf{1}_L \oplus \boldsymbol{a}_k, \tag{2}$$

Thus, all-one vector of length L is denoted by $\mathbf{1}_L$ and GF of addition is represented as $\oplus$ which operates as the addition-modulus. After a carrier frequency f_c is modulated by the MFSK modulator, the modulation signal is broadcasted over the channel. Specifically, let us suppose the transmitted signal k-th user is denoted as

$$s_k(t) = \sum_{l=0}^{L-1} \sqrt{2P_s} p(t - iT_s - lT_h) \times \exp[(2\pi(f_c + f_l^{(k)})t) + \phi_l^{(k)}], \tag{3}$$

where the transmitted power signal is P_s, the carrier frequency is f_c, the frequency tone is $f_l^{(k)}$ which is calculated by utilizing the information of X_k and $a_k(l)$, and the normalised pulse waveform is $p(t)$ having duration T_h. ϕ_l^k is the initialization phase for the MFSK. Now all the transmitted signals will be Inverse Fast Fourier Transformed (IFFT) and stored as a stream $\boldsymbol{s}$ vector, where $K \leq N_s$. The generator/transmitter side is associated with N_t^{RF} antenna chains and the RF beam-former matrix is $\boldsymbol{F}_{RF}$ of size

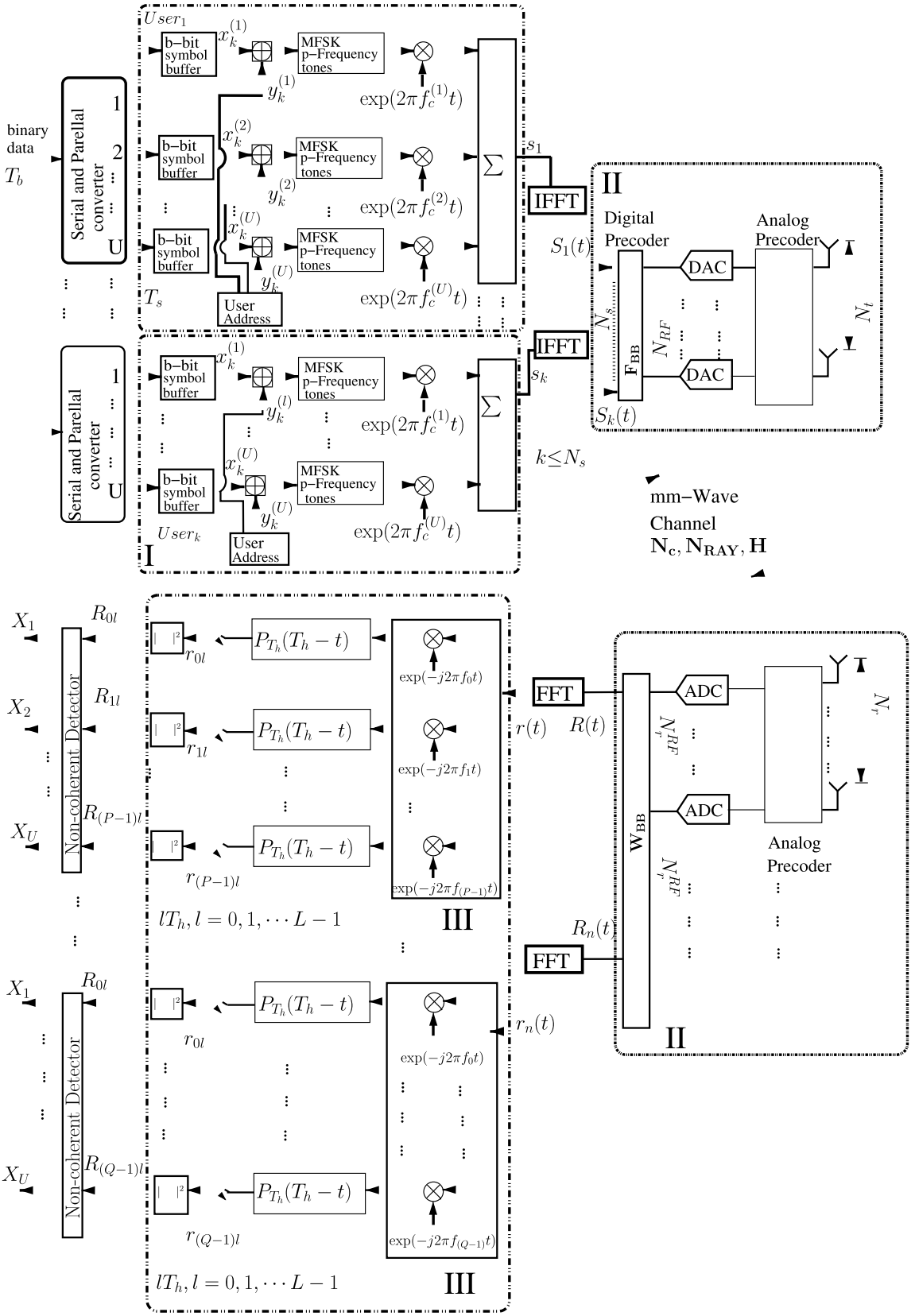

FIGURE 1. The detail configuration of our system model employed for the FFH scheme incorporated with mm-Wave.

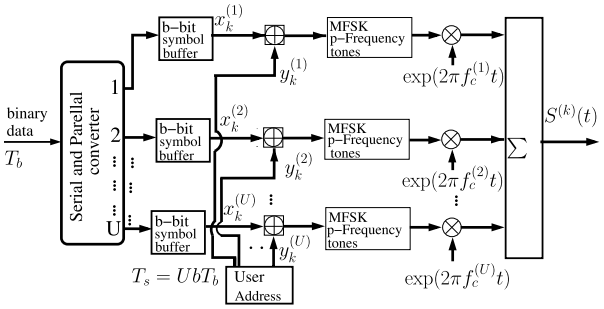

FIGURE 2. The transmitter schematic of the FFH model utilizing the MFSK modulation.

$N_t \times N_t^{RF}$. The base-band Transmit PreCoder (TPC) matrix side is denoted by $\boldsymbol{F}_{BB}$ having size $N_t^{RF`} \times N_s$, respectively.

III. mm-WAVE CHANNEL

The mm-Wave channel is employed with the widely used of multi-path system, in which a number of distribution paths are linked with a little scatters [4], [9], [19], [57]. The statistical channel model $\boldsymbol{H}$ response is represented as

$$\boldsymbol{H} = \sqrt{\frac{N_r N_t}{N_c N_{ray}}} \sum_{n_c=1}^{N_c} \sum_{n_{ray}=1}^{N_{ray}} \alpha_{n_c}^{n_{ray}} a_r(\phi_{n_c}^{n_{ray}}) \times (a_t^T(\phi_{n_c}^{n_{ray}})). \quad (4)$$

The statistical channel matrix $\boldsymbol{H}$ is of size $N_r \times N_t$ so that $\mathrm{E}[||H||_F^2] = N_t N_r$, while $\alpha_{n_c}^{n_{ray}}$ is the approximation to the complex-valued Gaussian random variable denoted by $\approx CN(0, 1)$, which has uniform distribution containing Rayleigh phase and amplitude. The response vector a_r and a_t of Uniform Linear Array (ULA) having antenna elements N_r and N_t are represented as:

$$a_r(\phi_r) = [1 \;\; e^{i\frac{2\pi}{\lambda} d\cos(\phi_r)} \;\; \ldots \;\; e^{i\frac{2\pi}{\lambda}(N_r-1)d\cos(\phi_r)}]^T, \quad (5)$$

$$a_t(\phi_t) = [1 \;\; e^{i\frac{2\pi}{\lambda} d\cos(\phi_t)} \;\; \ldots \;\; e^{i\frac{2\pi}{\lambda}(N_t-1)d\cos(\phi_t)}]^T. \quad (6)$$

IV. RECEIVED SIGNAL

Now considering a single mm-Wave model depicted in Fig. 1, where the receiver is provided with N_r receive antennas. After the RF and base-band combination the received signal vector is represented as

$$\boldsymbol{r} = \boldsymbol{W}_{BB}^H \boldsymbol{W}_{RF}^H \boldsymbol{H} \boldsymbol{F}_{RF} \boldsymbol{F}_{BB} \boldsymbol{s} + \boldsymbol{W}_{BB}^H \boldsymbol{W}_{RF}^H \boldsymbol{n}, \quad (7)$$

where the receiver side is linked with N_r^{RF} chains, the RF combiner matrix size is $N_r^{RF} \times N_r$ denoted by $\boldsymbol{W}_{RF}$, the base-band combiner having size $N_s \times N_r^{RF}$ denoted by $\boldsymbol{W}_{BB}$, respectively. The received vector is $\boldsymbol{y}$ of size N_s and the noise vector n of independent and identically distributed $CN(0, \sigma^2)$.

In Fig. 1 the mm-Wave based architecture is presented, where F_{RF} and W_{RF} are expressed as analogue BF. The beams are phase shifted, which are navigated and guided in the direction of the desired users. The base-band precoder are F_{BB} and combiner weights are W_{BB}, which are utilized for proliferating the inter-stream interference as indicated in

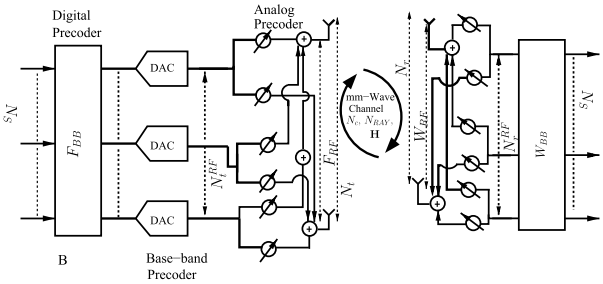

FIGURE 3. A hybrid precoding beamforming RF architecture design for full-array-based on mm-Wave system.

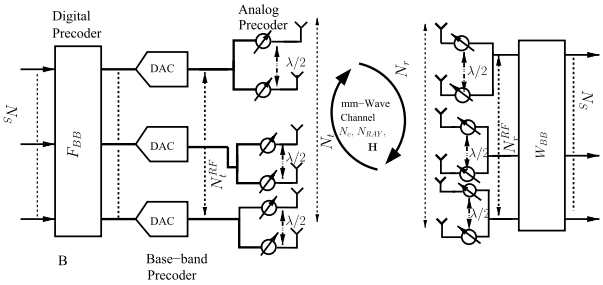

FIGURE 4. A hybrid precoding beamforming RF architecture design for sub-array-based on mm-Wave system.

Fig. 4. By utilizing this concept model, the achievable rate is expressed as:

$$C = \log_2 |det(I_{N_s} + \frac{P_s}{N_s} R_n^{-1} W_{BB}^H W_{RF}^H H F_{RF} F_{BB} F_{BB}^H F_{RF}^H W_{RF} W_{BB})| \; bits\ per\ second\ per\ channel\ use\ (bps/cu) \quad (8)$$

where $R_n = \sigma^2 W_{BB}^H W_{RF}^H W_{RF} W_{BB}$.

V. CODE-BOOK DESIGN

The TPC and analog BF transceiver design is shown in Figs. 3 and 4. In this design, the information data are precoded prior to the transmission. The base-band utilizing a linear TPC, then the RF beamformer precoded data are transferred. The data are transferred to the transmitted antennas through a phase shift procedure. The RF beamforming are assisted by the DFT, whereas antenna weights are chosen for obtaining desire navigation in the suitable aspect.

A. SUB-ARRAY DESIGN (SAD) CONNECTED ARCHITECTURES

In this design the base-band signal is precoded utilizing a linear TPC approach. The sub-arrays are separated by the full-connected array design which can be seen in Fig. 5. In the Sub-Array Design (SAD) approach, the sub-arrays are split according to the distance of $\lambda/2$ and individual RF chain is coupled with the sub-array for digital processing as illustrated in Fig. 5, so that the channel becomes geometrically correlated across all the antennas. This condition depends only on the Angle of Departure (AoD) of the signal at the transmitter, which is calculated in the Eq. 6 of transmitter

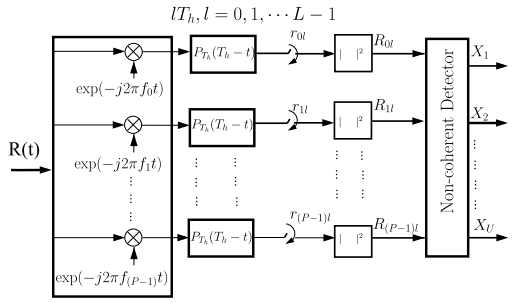

FIGURE 5. Receiver for the FFH aided non-coherent MFSK receiver using linear combining techniques.

antenna a_t^T. More importantly, the a_t^T is related to the function of AoD which is same when the full rank is greater than the channel matrix H thus making the channel correlated. This condition depends upon two factors, namely the distance between two sub-arrays should be less and the minimum separation distance should be $\lambda/2$ and other is the angular spread of the AoD. This is measured from one sub-array to another and should be small which effects the correlation of the given signal. Presuming that the sub-array i of the transmitter is transmitted through the H_i then the channel matrix is expressed as $H = [H_1, \ldots, H_{N_{RF}}]$, where each sub-channel H_i is correlated with $H_j \ \forall i \neq j$.

Please note that in full-array-connected design, the number of phase shifters needed is always greater than the SAD approach. Assuming that the transmit antennas N_t are connected to the RF chain N_t^{RF} so the full connected design requires $N_t \times N_t^{RF}$ phase shifters but the SAD would require only N_t phase shifters.

B. RF ANALOG BEAMFORMER DESIGN USING DFT

In mm-Wave the propagation losses are due to the foliage, oxygen absorption and water vapour thus by adopting BF we can reduce them. In BF case the antennas are separated by $\lambda/2$ distance [6], [8], [23], [61]. We explore the optimal beamforming weight vectors of the statistical distribution matches identically to the DFT based code-book for RF beamforming, making the correlated channel more effective and efficient in terms of DFT based code-book [44]. Moreover, the constant modulus helps in communication system to avoid power imbalanced, which is introduced by the phase shifters [24], [32]. Thus, utilizing the analog RF beamforming using phase shifters is sensible approach in DFT based code-book [24], [32], [44]. Beside, for the base band TPC matrix, we design a code-book which works on the principle of mutually unbiased bases (MUB)s to achieve maximum efficiency despite of having low complexity. The analog RF beamformer F_{RF} having a column of N_t^{RF} is obtained from the DFT matrix having size of $N_t \times N_t$, which reveals that the singular matrix of the channel $H = U \sum V^H$ has the maximum correlation at the extreme right side of the channel that is V and RF beamformer is expressed as

$$F_{RF}(:, i) = \max_i < DFT_{Nt}(:, i), V >, \quad 1 \leq i \leq N_t^{RF} \quad (9)$$

where the i^{th} column is $DFT_{Nt}(:, i)$ having DFT matrix $N_t \times N_t$, the right singular matrix of the channel is V. The column of W_{RF} are N_r^{RF} which are selected from the DFT matrix of order $N_r \times N_r$, this DFT column generates the maximum correlation of the channel H located at the left hand side of the singular matrix

$$W_{RF}(:, i) = \max_i < DFT_{Nr}(:, i), U >, \quad 1 \leq i \leq N_r^{RF} \quad (10)$$

where the i^{th} column is $DFT_{Nr}(:, i)$ having the $N_r \times N_r$ DFT matrix, the left singular matrix of the channel is U. Therefore, on the channel analog RF beamformer weights are applied by the base band TPC, the effective channel can be expressed as

$$H_{eff} = W_{RF}^H H F_{RF} \quad (11)$$

C. BASE-BAND CODE-BOOK DESIGN MUBs

The methodology of code-book design and MUB is explained in this passage. Let a set of orthonormal base of dimension N of Hilbert space are C and C'. According to the information given in [62], where C and C' are mutually unbiased if and only if this condition exists.

$$| < c, c' > |^2 = \frac{1}{N}, \quad \forall\, c \in C \text{ and } c' \in C' \quad (12)$$

Here c, c' are vectors belong to C and C' respectively. Thus, the number of MUBs is restricted in a given dimension, so that the code book build from MUBs should have a minimum distance as expressed in [44]. It is mandatory that the number of antennas should be in prime power as illustrated in [56], which leads to the information that the number of MUBs antennas expressed as N_t^{RF} having a dimension of $N_t^{RF} + 1$. By doing this the values of the MUB matrix will be of finite alphabets which are $1, -1, i, -i$. Moreover, if $F_1, \cdots, F_N$ are codewords then the distance between the two successive numbers should be minimum expressed in [44], [62] and given by

$$d_{min} = \min_{k,1:k\neq l} ||F_k F_k^H - F_l F_l^H|| \quad (13)$$

D. CODE BOOK CONSTRUCTION

For a code-book construction, we use a Hadamard Matrix D of dimension size 2^n where a natural number is n, which obeys the general condition of a MUB. Thus, utilizing the concept of Hadamard matrix D, we are generating a matrix E having same matrix size that of the D matrix. Now let us find the column vector v, by estimating/calculating the elements present in $C^H v$.[1] Now considering the concerned matrix D, where each element is obtained by element-wise multiplication of v with C where $C = c_1, c_2, \ldots, c_{2^n}$ so our concern matrix $D = v \otimes C_{2^n} = [vc_1, vc_2, \ldots, vc_{2^n}]$. This process will be continued until all the $2^n + 1$ values are obtained for the calculations. Now let us consider the system where we have four transmitted antennas so the RF becomes

[1] where the magnitude is equal to 1.

$N_t^{RF} = 4$ and the Hadamard matrix C becomes

$$C = \frac{1}{2}\begin{bmatrix} 1 & 1 & 1 & 1 \\ 1 & 1 & -1 & -1 \\ 1 & -1 & -1 & 1 \\ 1 & -1 & -1 & 1 \end{bmatrix} \tag{14}$$

The above equation containing $\frac{1}{2}$ satisfies the basic concept of [55]. The vector v_1 is selected as the magnitude of all the elements becomes equal to 1 when we achieve all the calculation of $A^H v_i$. For the solution, we assume following three possibilities

$$v_1 = \begin{bmatrix} 1 \\ -1 \\ -i \\ i \end{bmatrix}, \quad v_2 = \begin{bmatrix} 1 \\ -i \\ -i \\ -1 \end{bmatrix}, \quad v_3 = \begin{bmatrix} 1 \\ i \\ 1 \\ -i \end{bmatrix} \tag{15}$$

Now solving the above equation we get the set of MUBs which are given by $D = v_1 \otimes C, E = v_2 \otimes C$, and $F = v_3 \otimes C$,

$$D = \frac{1}{2}\begin{bmatrix} 1 & 1 & 1 & 1 \\ -1 & -1 & 1 & 1 \\ -i & i & i & -i \\ -i & i & -i & i \end{bmatrix},$$
$$E = \frac{1}{2}\begin{bmatrix} 1 & 1 & 1 & 1 \\ -i & -i & i & i \\ -i & i & i & -i \\ -1 & 1 & -1 & 1 \end{bmatrix},$$
$$F = \frac{1}{2}\begin{bmatrix} 1 & 1 & 1 & 1 \\ i & i & -i & -i \\ 1 & -1 & -1 & 1 \\ -i & i & -i & i \end{bmatrix}, \tag{16}$$

Since the results obtained from the above Eqs. illustrates that we have identical matrix which satisfies all the condition of [55]. Therefore, obtaining the MUBs $N_t^{RF} + 1 = 5$, the input streams are non-linear, hence the linear process cannot occur in the identity matrix, so we need to dumped the feedback overhead. The left circular shift of each matrix will obtain the code-book entries for the concern matrices C, D, E, F as we are doing 4 shifts so $C = 2^4 = 16$ entries will be there. Therefore, the set of TPC matrices will have following entries for the code book

$$C_A = C_0, C_1, C_2, C_3, D_0, D_1, D_2, D_3, E_0, E_1, E_2, E_3, F_0, F_1, F_2, F_3. \tag{17}$$

After obtaining the code-book C_A, we select and obtain the first column of the specific TPC matrix having the minimum SNR of all the links of transceiver design of the concerned channel

$$SNR_k = \frac{P}{N_s N_0 (F_{BB}^* H_{eff}^* H_{eff} F_{BB})_{kk}^{-1}} \tag{18}$$

where the concerned noise power is expressed as N_0 and the signal power is P respectively. Therefore, the TPC F_{BB} which encounters the minimum SNR is selected by the code-book C_A which obeys

$$F_{BB} = \arg \max_{F_{BB} \in C_A} \Lambda_{min} H_{eff} F_{BB} \tag{19}$$

where the minimum singular value is Λ_{min} of $H_{eff} F_{BB}$. Moreover, the mm-Wave channel is correlated when $\lambda/2$ is the space between two adjacent antenna elements. Therefore using MUB based TPC structure with DFT assisted RF BF minimizes the intricacy, thus improving the performance in spatially correlated channel.

The idea of our design pseudo code is listed in Algorithm 1:

Algorithm 1 Design of Code-Book for RF and Base-Band

Acquiring the code-book C_A and restoring it in a memory

1) Obtain the vector v_i by the method of Hadamard matrix $D_{N_t}^{RF}$ such that the magnitude of all elements of $D^H V_i = 1$;
2) Obtaining MUBs by multiplying element by element-wise of V_i such that $D, \forall\ 1 \leq i \leq (N_t^{RF} - 1)$;
3) The code-book C_A is obtained by performing the left circular shift of every MUB to x locates, thus $x = 1, \cdots, N_t^{RF} - 1$;

Following mechanism helps in the selection of TPC from the code-book

1) **By knowing the information about the $H = U \sum V^H$;**
2) **Achieving the desire columns of F_{RF} and W_{RF} from DFT_N so that $F_{RF} = \max < DFT_{N_t}(:, i), V >$, $1 \leq i \leq N_t^{RF}$ and $W_{RF} = \max < DFT_{N_r}(:, i), U >$, $1 \leq i \leq N_r^{RF}$.**
3) **Then the effective channel is $H_{eff} = W_{RF}^H H F_{RF}$**
4) **Picking the desire TPC from the code-book which convince the $F_{BB} = \arg \max_{F_{BB} \in C_A} \Lambda_{min} H_{eff} F_{BB}$;**
5) **The Zero Force (ZF) combiner is W_{BB}.**

The complexity in the code-book is related to the number of estimations needed for achieving and obtaining the best TPC matrix. For achieving the TPC matrix from the code-book we need to calculate and accomplish $CN_r^{RF}(N_t^{RF} - 1)$ which is complex valued addition as expressed in [60], [63], the cardinality of the code-book is C. Note that its complex value addition and it cannot treated as complex multiplication. Where as, when the Grassmannian and Fourier design are used, we need to perform complex multiplication plus addition. Thus, we obtained $CN_s(N_r^{RF})^2$ plus $C(N_r^{RF})^2$ $(N_s - 1)$ as illustrated by [61]. Moreover, using TPC in the base-band we operates on perfect CSI, such that utilizing similar number of RF chains and only if we utilized to use complex value $N_s N_r^{RF}(N_t^{RF} - 1)$ addition plus the multiplication of $N_s N_r^{RF}(N_t^{RF} - 1)$ which shows that the MUBs based code-book design reduces overall complexity when using it in the BF structure. Hence, the values of code-book are made from a finite alphabets $\Im = i, -i, 1, -1$, which has constant modulus constraints and thus helps in

providing the power imbalance to the system. Please note that the computation performed by the transmission of the higher rank are associated with the code-book, which is reused for the transmission of lower rank systems, as they are subset of the higher rank transmission.

VI. FFH NON-COHERENT MFSK RECEIVER

We examine the behaviour of an FFH aided non-coherent MFSK receiver utilizing linear combining scheme for perceiving the generated signal as shown in Fig. 1. If the generated signal is mitigated by the noise and passes through the interference-free channel, then during the l^{th} hop duration T_h the signal received is represented as

$$R(t) = \sum_{k=1}^{K} \sqrt{2P} \sum_{l=0}^{L-1} h_l^{(k)} P_{Th}(t - lT_h) \exp(2\pi f_l(k)t) + N(t) \tag{20}$$

The channel gain is expressed as $h_l^{(k)}$ which corresponds to the k^{th} user for the frequency as $f_l^{(k)}$ and the complex Additive White Gaussian Noise (AWGN) is represented as $N(t)$ having zero mean. The noise power spread over the complete spread spectrum bandwidth of R is N_0 times B. Therefore, the signal power P to the noise power ratio over the full hopping bandwidth R is expressed as

$$SNR = \frac{P}{\sigma_N^2} = \frac{E_s}{T_s N_0 B} = \frac{E_s}{LT_h N_0 MNR} \tag{21}$$

where the energy per transmitted symbol is E_s, the transmitted symbol duration is $T_s = LT_h$ and FSK signal bandwidth is denoted by $R = \frac{1}{T_h}$. The signal noise power ratio over a single frequency band of M-MFSK tones is given by E_s/LN_0 and than corresponding to a single FSK signal having a bandwidth is B may be expressed as E_s/LN_0.

In Fig. 5 the MFSK detector preventing the decision making as shown having non-coherent detection. It is visualized that after some normalisation the samples of input can be expressed as

$$R_{ml} = |r_{ml}|^2 = |\sum_{k=1}^{K} h_m^{(k)} \delta[y_k(l), m] + n_{ml}|^2$$
$$m = 0, 1, \cdots, P-1; \quad l = 0, 1, \cdots, L-1 \tag{22}$$

where Dirac Delta function is $\delta[x, y]$ which exist as $\delta[x, x] = 1$ and $\delta[x, y] = 0$ for $x \neq y$, complex Gaussian noise sample distributed with zero mean is n_{ml} and a variance $\sigma^2 = LN_0/E_s$, where the energy per MFSK symbol is denoted as $E_s = PT_s$. In Fig. 5, the non-coherent detector is either a single user detector or multi user detector, which operates on the hard decision criteria as done in [24], [64]. Referring to Fig. 5, where linear combination model is used to integrate all the hops available in the signal. The decision variables are computed by the diversity combiner output M. The decision is gathered on the principle of highest magnitude value referred as Maximum Likelihood (ML). The decision index variable generates the estimation of the transmitted symbols. A decision error can occur only if the decision amplitude corresponds to the non-signal tones, which refers to the one tone which exceeds the transmitted signal tone.

$$U_{0l} = (r_{0,c})^2 = PT_h + n_0 = E_h + N_0 \tag{23}$$

where the AWGN components are $N_0 = N_{0c}^2 + N_{0s}^2$ respectively. The output of the detector associates with the generated signal tone as expressed in Eq. (23) and the remaining $(P-1)$ detectors associate with non-signal tones, it is envisioned that thermal noise can mitigate its output by performing superposition principle. Therefore it is expressed as

$$U_{m,l} = u_m, \quad where\ m > 0 \tag{24}$$

The above Eq. (24) reveals that the output is mitigated by noise and the interference present in the signal which effects all the tones M present in the band.

$$U_{0,l} = E_h + n_0 \quad \text{and} \tag{25}$$
$$U_{ml} = n_m \quad m > 0 \tag{26}$$

Accordingly, the noise mitigates the signal and it significantly deteriorates the signal. In the scenario of FFH models, all the hops experience noise and jamming independently whereas jamming is low to overcome this linear combination scheme is utilized.

1) TRANSMITTER SIDE

The generated signal of the k^{th} user is represented as

$$S_k(t) = \sum_{i=0}^{L-l} \sqrt{2P} P_{Th}(t - iT_s - lT_h) \times \exp(2\pi[f_k + f_1^{(k)}]t + \phi_l^{(k)}) \tag{27}$$

Here, the transmitted power is expressed as 'P', the rectangular pulse-shaped signalling waveform is expressed as $P_{Th(t)}$ which is linked with a chip time interval as the phase $\phi_l^{(k)}$ introduced by MFSK.

2) RECEIVER SIDE

The signal $s(t)$ is modulated by BFSK over a mm-Wave fading channel which is expressed at the receiver side by

$$r(t) = \alpha e^{-\phi} s(t) + n(t) \tag{28}$$

where the Rayleigh distribution is expressed as α as shown in Eq. 28. The channel-induced phase shift is expressed as ϕ in the generated signal and the Gaussian Distribution Noise is denoted by $n(t)$. The first symbol interval is generated by the l^{th} tone. The received signal without noise is denoted as

$$r(t) = \sqrt{2P} \exp[2\pi(f_k + f_l)t + \phi_l] \quad 0 \leq t \leq T_s \tag{29}$$

Now combining the generated signal by the k^{th} user's without the noise is denoted as

$$r(t) = \sum_{k=0}^{K} \sqrt{2P} \sum_{l=0}^{L-1} P_{Th}(t - iT_s - lT_h - \tau_k) \times \exp([2\pi[f_k + f_1^{(k)}]t + \phi_l^{(k)}) \tag{30}$$

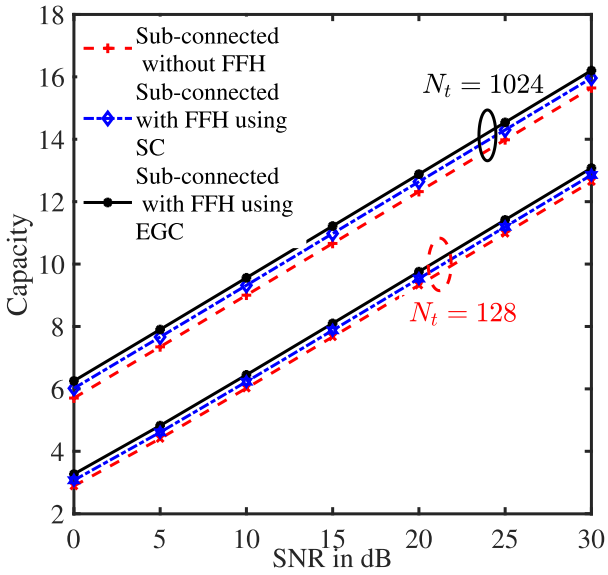

FIGURE 6. Outage capacity $p_{out} = 1\%$ for Sub-array-connected system for $N_t = 128$, 1024 antennas with and without FFH system.

where the time delay is τ_k for the k^{th} user. Let us suppose a signal is corrupted by a noise in the system, thus making it difficult to predict the unwanted signal because of its random behaviour [24], [65]. It is often narrated as that noise is one of the major factor which effect the signal directly [24], [65], so in other words the generated signal are affected by noise independently. Therefore, the received signal are expressed as

$$r(t) = \sum_{k=0}^{K} \sqrt{2P} \sum_{l=0}^{L-1} h_l^k P_{Th}(t - lT_h - \tau_k) \times \exp([2\pi f_1^{(k)} t] + N(t) \quad (31)$$

where, the AWGN is expressed as N(t). It can be noted that the receiver for FFH signal is inverse structure of the transmitter of Fig. 2. The FH pattern is utilized to perform down conversion for the received signal which is multiplied by the carrier frequency as illustrated in Fig. 6. Referring to Fig. 6, the signal is first transferred to a bank of energy detector, where the MFSK procedure is used to convert the obtained signal which is referred to down converted signal. The signal received, uses the identical information as that of the transmitted signal. Please note that the FH intervals of the desired user are synchronized with the detection interval FH time as expressed by T_h. The energy detectors of M produce a output of $M \times L$, where L chips are associated with M-ary symbol interval of T_s second. In Fig. 2 at the transmitter side MFSK signal converts a 'b' bit symbol to the unique sequence which is called as user address. The output Y_k is received at the receiver, where as energy detection is performed to obtain the generated symbol of X_k belonging to k^{th} user, where modulo two is carried out to generate the output. The purpose of this is to subtract the user address a_k from the Y_k information. Thus, leading to the equation.

$$Y_k - a_k = X_k l + 0 = X_k.1 \quad (32)$$

where the vector of the length L have zero value. The time frequency matrices dimension is $M \times L$ where rows are M and columns are L, which describes the detection of the user address at the receiver. The MFSK frequency stages has M rows having bandwidth R_h and L narrates the corresponding chips having time duration T_h and symbol time interval T_s. The identical user-address $a_k = [5, 2, 6, 4]$ is used at the receiver out $Y_k = [0, 5, 1, 7]$ where as the same user-address is used for de-hopping.

VII. SIMULATION RESULTS

The performance of our FFH in mm-Wave channels is evaluated in this section. Our analysis compares the performance results with and without FFH for mm-Wave communication. Before evaluating the Probability of Error P_e, we quantify the outage capacity, using DFT-MUB matrix in mm-Wave system by considering operation in both the FFH and non-FFH mode. According to Shannon Capacity, the system works well with finite error probability by utilizing finite blocks for the estimation of the system. By contrast if the infinite block length are used then the outage capacity is calculated which achieves better performance as compared with the finite block lengths of Shannon work [60], [66], [67]. Therefore, to visualize the system, we calculated the outage capacity.

A. OUTAGE CAPACITY

The model is said to be in outage condition only if, when at a given threshold rate the data rate falls below it as illustrated by [66], [67]. The Shannon capacity is measured in [46], which fall below the threshold rate of C_{out}. Moreover, the outage probability p_{out} is calculated by the outage capacity as

$$p_{out} = \mathrm{P}(log_2(1 + ||h||^2 SNR) < C_{out}), \quad (33)$$

where the probability is denoted by P, the Rayleigh distribution of fading is h and the sum of squares of random variables having the distribution of Chi-square is given by $||h||^2$ with degree of freedom by $2N_{sub}$, where N_{sub} is the number of sub-arrays present in the system. Accordingly [66] the above Eq. (33) becomes as

$$p_{out} = \mathrm{P}(||h||^2 SNR) < \frac{2^{C_{out}-1}}{SNR}. \quad (34)$$

Now the p.d.f of $||h||^2$ becomes $\frac{1}{(N_{sub}-1)!} h^{N_{sub}^{-1}} e^{-h}$, $h \geq 0$, where the high SNRs are achieved according to [24] the above Eq. (34) becomes

$$p_{out} = \frac{(2^{C_{out}-1)^{N_{sub}}})}{N_{sub}! SNR^{N_{sub}}}, \quad (35)$$

where $SNR = \frac{N_t \mathrm{P}}{N_{sub}^2 N_0}$, $\frac{N_t}{N_{sub}}$ deals with the beam forming while the power allocation for all the sub-branches is $\frac{1}{N_{sub}}$. Fig. 6 depicts an outage capacity versus given SNR, when the outage probability is fixed to $p_{out} = 1\%$. In this figure, FFH is employed using two combining schemes such as

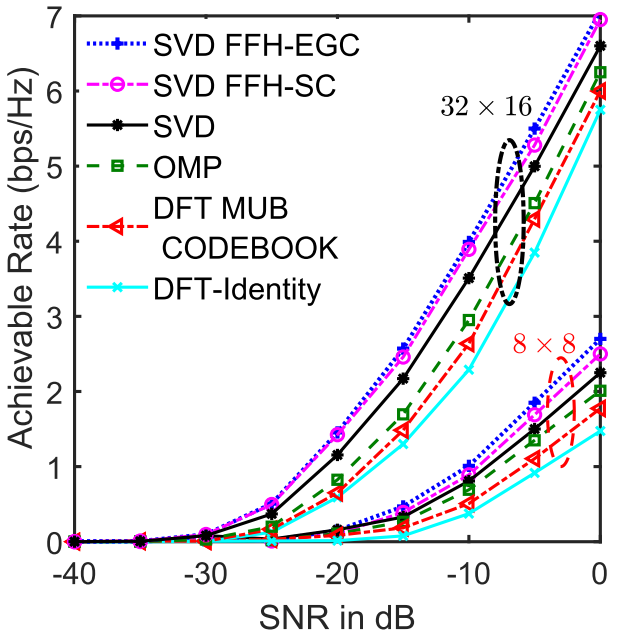

FIGURE 7. Achievable rate utilizing DFT-MUB based code-book model for 4-bit feedback system, and with unconstrained precoder for model 8 × 8 and 32 × 16 sub-connected MIMO configuration.

the Equal Gain Combiner (EGC) and the Selective gain Combiner (SC). We have also compared the performance of the mm-Wave system when FFH is not employed. We have also incorporated different number of transmit antennas such as $N_t = 128$ and 1024. It can be observed from the figure that as the number of transmit antennas increases the performance becomes better because of the transmit diversity gain. Furthermore, the EGC scheme outclass the SC scheme for a given SNR. This improvement is because EGC employs co-phases the signals of each branch and then combines them with equal weighting. While the SC only combines the output branch which has the highest SNR. From the result of Fig. 6, it can be deduced that FFH can be employed for sub-array architecture for mm-Wave system.

B. ACHIEVABLE RATE

We analyse the achievable rate while using the Sub-connected Array using FFH system in mm-Wave model. The Monte Carlo simulation are performed for evaluating the achievable rates of linear combination scheme of EGC utilizing SVD, SC utilizing SVD, unconstrained digital precoding utilizing SVD, Orthogonal Matching Pursuit (OMP), DFT-MUB code-book and DFT-Identity, for 8 × 8 and 32 × 16 MIMO systems. For DFT-Identity precoder, the identity matrix is selected as the baseband TPC are depicted in Fig. 7. 4-bit feedback is evaluated for the DFT-MUB based code-book model. From Fig. 7, there remains a gap between the SVD based EGC, SC, TPC and the DFT-MUB based code-book which is around 3 *dB* for 32 × 16 and as low as 1.0 dB for 8 × 8 MIMO configurations. Moreover, there is a gap of about 1.1 dB versus the OMP aided precoding model for 32 × 16 MIMO, whereas the performance of

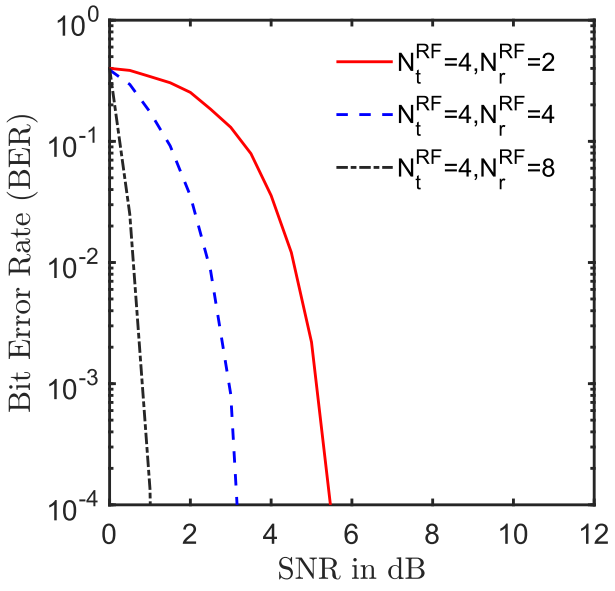

FIGURE 8. Comparison of uncoded BER of a 8 × 8 amongst the DFT-MUB aided code-book model.

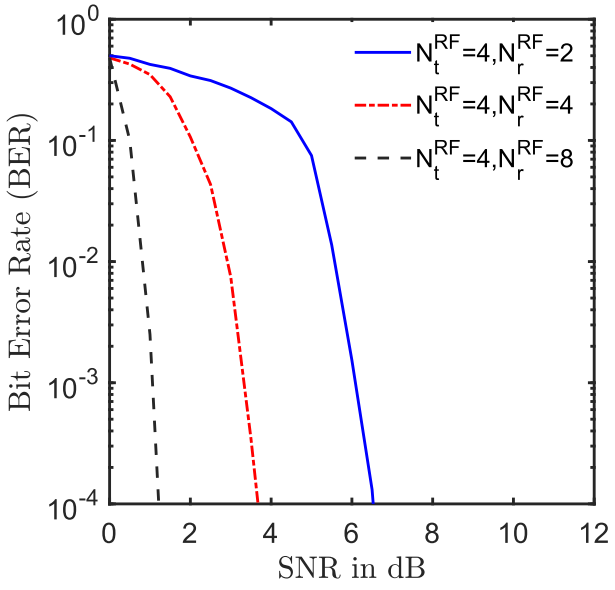

FIGURE 9. BER performance of FFH/MFSK system employed in mm-Wave channel having different receiving antennas.

DFT-MUB for 8 × 8 MIMO matches with the OMP. The comparison between all these schemes are carried out in mm-Wave channel using DFT-Identity aided model, here the TPC is formulated by choosing first N_s columns of the identity matrix. Approximately 0.72 dB gain is calculated while using DFT-MUB with DFT-Identity aided model. Identical performance is obtained for the DFT-Identity and DFT-MUB, as the channel is correlated, beside the performance gain of the MUB code-book is marginally correlated in the base-band channels.

Fig. 8, depicts the BER performance results of SC, when deployed in FFH system using mm-Wave channel. We evaluated the performance gap between the SC through Monte Carlo simulation. In this configuration, received

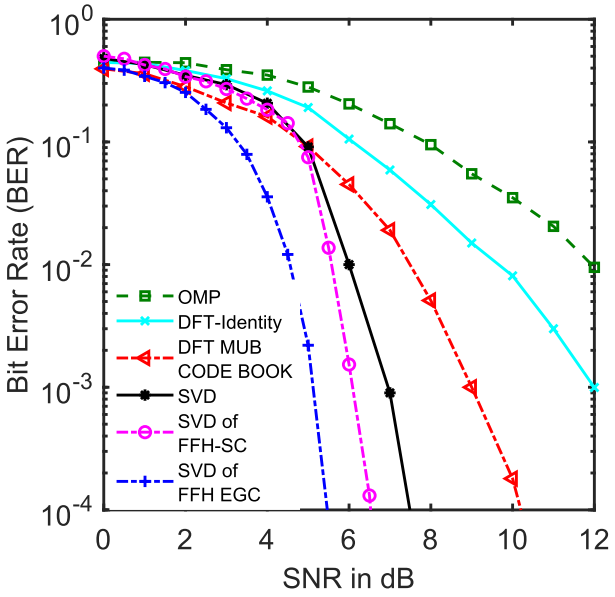

FIGURE 10. Comparison of BER performance of FFH system using EGC, SC with the state of art scheme used in mm-Wave system having of a 8 × 8 DFT MUB based code-book design.

antennas can be varied while keeping transmit antennas fixed. A 3 dB gain is obtained by varying receiving antennas from $2- > 8$. We see that SVD of each system behave better when employed in FAAS system. It is observed that adopting FFH schemes in mm-Wave system with employing the DFT-MUB code book. The FFH behave better, when $N_r = 8$ we achieve 3 *dB* gain in a particular SNR and when system parameters are same we achieve almost 1 dB we have one entry for detecting $M \times L$ entries. Fig. 8, depicts that by using FFH system, we can achieve better gains despite of little system complexity.

Fig. 9 demonstrates that the performance of EGC when deployed in mm-Wave channel. In Fig. 9 when we employ more antennas we achieve a better gain. In Fig. 9, transmitter antennas are fixed and receiving attennas varies. We achieve better gain as soon as more antennas are deployed at the receiver. In this respect, we attain 3 *dB* gain when N_t^{RF} are increased from 2 to 8. This result indicates that diversity is gained because of two factors namely, the antennas increased at the receiver and other linear combination schemes.

Fig. 10 shows that the EGC attains better BER performance versus the other schemes used in mm-wave channel. Furthermore, it can be observed that FFH EGC-SVD at 10^{-4} BER achieves 6 *dB* where as FFH SC-SVD achieves 7 *dB*, unconstrained SVD mm-Wave achieves 8 *dB* and DFT-MUB code-book is around 12 *dB* which indicates that the FFH EGC-SVD performs better and obtain better gain because of diversity gain as at lower SNR FFH-SVD SC and SVD of DFT-MUB code book behave better. Moreover, with BER at 10^{-4} the performance gap between unconstrained SVD, SVD of SC and SVD of EGC become more because at higher SNR values we get better maximum values of U_m has at these values of SNR we achieves optimum number of entries to eliminate from individual rows in the detection matrix, which results in best performance than EGC.

VIII. CONCLUSION

A hybrid code-book model is evaluated with the aid of the MUB base-band and RF in the DFT. The FFH model is utilized for mm-Wave channel. We demonstrated that the proposed design exhibits progressive performance in the form of achievable rate and moreover, we achieve better gains which is within 2 to 3 *dB* from the SVD precoding. The scheme imposes significantly low complexity than OMP and SVD. A novel design is proposed for the FFH model, which caters for mitigating the fading environment for mm-Wave channels. Moreover, simulations demonstrate that by utilizing FFH model we attain better gain than the existing schemes in the mm-Wave channel. It was demonstrated that the FFH system provides extra diversity gain when employed in BF. Finally, the DFT-MUB code-book is obtained on the contrary of the FFH system model in order to estimate how much gain is achieved in-terms of achievable rate and outage capacity. It was observed that by adopting linear combination schemes in FFH system, we achieve better gain and better outage capacity then that of conventional mm-Wave system. EGC performs better than SC combiner when used in FFH system.

REFERENCES

[1] K. Ying, Z. Gao, S. Lyu, Y. Wu, H. Wang, and M. Alouini, "GMD-based hybrid beamforming for large reconfigurable intelligent surface assisted millimeter-wave massive MIMO," *IEEE Access*, vol. 8, pp. 19530–19539, 2020.

[2] Z. Wan, Z. Gao, B. Shim, K. Yang, G. Mao, and M.-S. Alouini, "Compressive sensing based channel estimation for millimeter-wave full-dimensional MIMO with lens-array," *IEEE Trans. Veh. Technol.*, vol. 69, no. 2, pp. 2337–2342, Feb. 2020.

[3] O. Alluhaibi, Q. Z. Ahmed, E. Kampert, M. D. Higgins, and J. Wang, "Revisiting the energy-efficient hybrid D–A precoding and combining design for mm-wave systems," *IEEE Trans. Green Commun. Netw.*, vol. 4, no. 2, pp. 340–354, Jun. 2020.

[4] T. S. Rappaport, Y. Xing, O. Kanhere, S. Ju, A. Madanayake, S. Mandal, A. Alkhateeb, and G. C. Trichopoulos, "Wireless communications and applications above 100 GHz: Opportunities and challenges for 6G and beyond," *IEEE Access*, vol. 7, pp. 78729–78757, 2019.

[5] J. Ferguson-Mitchell and F. Werner. "New ITU-T report consolidates views of wireless and transport communities," ITU Corporate Commun., Tech. Rep. ITU-R M. 2412-0, 2017. [Online]. Available: https://www.itu.int/en/about/Pages/default.aspx

[6] T. S. Rappaport, S. Sun, R. Mayzus, H. Zhao, Y. Azar, K. Wang, G. N. Wong, J. K. Schulz, M. Samimi, and F. Gutierrez, "Millimeter wave mobile communications for 5G cellular: It will work!" *IEEE Access*, vol. 1, pp. 335–349, 2013.

[7] I. A. Hemadeh, M. El-Hajjar, S. Won, and L. Hanzo, "Multi-set space-time shift keying and Space- frequency space-time shift keying for millimeter-wave communications," *IEEE Access*, vol. 5, pp. 8324–8342, 2017.

[8] I. A. Hemadeh, K. Satyanarayana, M. El-Hajjar, and L. Hanzo, "Millimeter-wave communications: Physical channel models, design considerations, antenna constructions, and link-budget," *IEEE Commun. Surveys Tuts.*, vol. 20, no. 2, pp. 870–913, 2nd Quart., 2018.

[9] J. Harvey, "Exploiting high millimeter wave bands for military communications, applications, and design," *IEEE Access*, vol. 7, pp. 52350–52359, 2019.

[10] Q.-U.-A. Nadeem, A. Kammoun, and M.-S. Alouini, "Elevation beamforming with full dimension MIMO architectures in 5G systems: A tutorial," *IEEE Commun. Surveys Tuts.*, vol. 21, no. 4, pp. 3238–3273, Jul. 2019.

[11] K. B. Letaief, W. Chen, Y. Shi, J. Zhang, and Y.-J.-A. Zhang, "The roadmap to 6G: AI empowered wireless networks," *IEEE Commun. Mag.*, vol. 57, no. 8, pp. 84–90, Aug. 2019.
[12] Y. Huo, X. Dong, W. Xu, and M. Yuen, "Enabling multi-functional 5G and beyond user equipment: A survey and tutorial," *IEEE Access*, vol. 7, pp. 116975–117008, 2019.
[13] G. Fettweis and S. Alamouti, "5G: Personal mobile internet beyond what cellular did to telephony," *IEEE Commun. Mag.*, vol. 52, no. 2, pp. 140–145, Feb. 2014.
[14] T. S. Rappaport, G. R. Maccartney, M. K. Samimi, and S. Sun, "Wideband millimeter-wave propagation measurements and channel models for future wireless communication system design," *IEEE Trans. Commun.*, vol. 63, no. 9, pp. 3029–3056, Sep. 2015.
[15] H. Elayan, O. Amin, B. Shihada, R. M. Shubair, and M.-S. Alouini, "Terahertz band: The last piece of RF spectrum puzzle for communication systems," *IEEE Open J. Commun. Soc.*, vol. 1, pp. 1–32, 2020.
[16] O. El Ayach, S. Rajagopal, S. Abu-Surra, Z. Pi, and R. W. Heath, Jr., "Spatially sparse precoding in millimeter wave MIMO systems," *IEEE Trans. Wireless Commun.*, vol. 13, no. 3, pp. 1499–1513, Mar. 2014.
[17] A. Alkhateeb, O. El Ayach, G. Leus, and R. W. Heath, Jr., "Channel estimation and hybrid precoding for millimeter wave cellular systems," *IEEE J. Sel. Topics Signal Process.*, vol. 8, no. 5, pp. 831–846, Oct. 2014.
[18] R. W. Heath, Jr., N. González-Prelcic, S. Rangan, W. Roh, and A. M. Sayeed, "An overview of signal processing techniques for millimeter wave MIMO systems," *IEEE J. Sel. Topics Signal Process.*, vol. 10, no. 3, pp. 436–453, Apr. 2016.
[19] Q. Sultan, M. S. Khan, and Y. S. Cho, "Fast 3D beamforming technique for millimeter-wave cellular systems with uniform planar arrays," *IEEE Access*, vol. 8, pp. 123469–123482, 2020.
[20] J. Zhang, E. Bjornson, M. Matthaiou, D. W. K. Ng, H. Yang, and D. J. Love, "Prospective multiple antenna technologies for beyond 5G," *IEEE J. Sel. Areas Commun.*, vol. 38, no. 8, pp. 1637–1660, Aug. 2020.
[21] M. Wenyan, Q. Chenhao, Z. Zhang, and J. Cheng, "Sparse channel estimation and hybrid precoding using deep learning for millimeter wave massive MIMO," *IEEE Trans. Commun.*, vol. 68, no. 5, pp. 2838–2849, Feb. 2020.
[22] W. B. Abbas, F. Gomez-Cuba, and M. Zorzi, "Millimeter wave receiver efficiency: A comprehensive comparison of beamforming schemes with low resolution ADCs," *IEEE Trans. Wireless Commun.*, vol. 16, no. 12, pp. 8131–8146, Dec. 2017.
[23] X. Gao, L. Dai, S. Han, I. Chih-Lin, and R. W. Heath, Jr., "Energy-efficient hybrid analog and digital precoding for mmWave MIMO systems with large antenna arrays," *IEEE J. Sel. Areas Commun.*, vol. 34, no. 4, pp. 998–1009, Apr. 2016.
[24] L. L. Yang, *Multicarrier Communication*. Hoboken, NJ, USA: Wiley, 2009.
[25] J. G. Proakis, *Digital Communication*, vol. 4, 4th ed. New York, NY, USA: McGraw-Hill, 2001.
[26] S. Luo, S. Zhang, S. Ke, S. Wang, X. Bu, and J. An, "Optimum combining for coherent FFH/DS spread spectrum receivers in the presence of multi-tone jammer," *IEEE Access*, vol. 8, pp. 53097–53106, 2020.
[27] K. A. Hamdi and L. Pap, "A unified framework for interference analysis of noncoherent MFSK wireless communications," *IEEE Trans. Commun.*, vol. 58, no. 8, pp. 2333–2344, Aug. 2010.
[28] F. Yang and L. L. Yang, "A single-user noncoherent combining scheme achieving multiuser interference mitigation for FFH/MFSK systems," *IEEE Trans. Wireless Commun.*, vol. 12, no. 9, pp. 4306–4314, Sep. 2013.
[29] S. Ahmed, L. L. Yang, and L. Hanzo, "Mellin-transform-based performance analysis of FFH M-ary FSK using product combining for combatting partial-band noise jamming," *IEEE Trans. Veh. Technol.*, vol. 57, no. 5, pp. 2757–2765, Sep. 2008.
[30] M. Chiani and A. Giorgetti, "Coexistence between uwb and narrow-band wireless communication systems," *Proc. IEEE*, vol. 97, no. 2, pp. 231–254, Feb. 2009.
[31] D. Goodman, P. Henry, and V. Prabhu, "Frequency-hopped multilevel FSK for mobile radio," *Bell Syst. Tech. J.*, vol. 59, no. 7, pp. 1241–1255, Sep. 1980.
[32] B. W. Adams, "Area communications system," U.S. Patent 5 034 961, Jul. 23, 1991.
[33] D. J. Goodman, "Cellular packet communications," *IEEE Trans. Commun.*, vol. 38, no. 8, pp. 1272–1280, Aug. 1990.
[34] J. Lee, R. French, and L. Miller, "Probability of error analyses of a BFSK frequency-hopping system with diversity under partial-band jamming interference-part I: Performance of square-law linear combining soft decision receiver," *IEEE Trans. Commun.*, vol. COM-32, no. 6, pp. 645–653, Jun. 1984.
[35] J. Lee and L. Miller, "Error performance analyses of differential phase-shift-keyed/frequency-hopping spread-spectrum communication system in the partial-band jamming environments," *IEEE Trans. Commun.*, vol. COM-30, no. 5, pp. 943–952, May 1982.
[36] J. Lee, L. Miller, and Y. Kim, "Probability of error analyses of a BFSK frequency-hopping system with diversity under partial-band jamming interference-part II: Performance of square-law nonlinear combining soft decision receivers," *IEEE Trans. Commun.*, vol. COM-32, no. 12, pp. 1243–1250, Dec. 1984.
[37] L. Miller, J. Lee, and A. Kadrichu, "Probability of error analyses of a BFSK frequency-hopping system with diversity under partial-band jamming interference-part III: Performance of a square-law self-normalizing soft decision receiver," *IEEE Trans. Commun.*, vol. COM-34, no. 7, pp. 669–675, Jul. 1986.
[38] Y.-S. Shen and S.-L. Su, "Performance analysis of an FFH/BFSK receiver with ratio-statistic combining in a fading channel with multitone interference," *IEEE Trans. Commun.*, vol. 51, no. 10, pp. 1643–1648, Oct. 2003.
[39] J. Wang and C. Jiang, "Analytical study of FFH systems with square-law diversity combining in the presence of multitone interference," *IEEE Trans. Commun.*, vol. 48, no. 7, pp. 1188–1196, Jul. 2000.
[40] K. C. Teh, A. C. Kot, and K. H. Li, "Error probabilities of an FFH/BFSK self-normalizing receiver in a rician fading channel with multitone jamming," *IEEE Trans. Commun.*, vol. 48, no. 2, pp. 308–315, Feb. 2000.
[41] C. Pan, H. Zhu, N. J. Gomes, and J. Wang, "Joint precoding and RRH selection for user-centric green MIMO C-RAN," *IEEE Trans. Wireless Commun.*, vol. 16, no. 5, pp. 2891–2906, May 2017.
[42] M. Agiwal, A. Roy, and N. Saxena, "Next generation 5G wireless networks: A comprehensive survey," *IEEE Commun. Surveys Tuts.*, vol. 18, no. 3, pp. 1617–1655, Feb. 2016.
[43] I. A. Hemadeh, M. El-Hajjar, and L. Hanzo, "Hierarchical multi-functional layered spatial modulation," *IEEE Access*, vol. 6, pp. 9492–9533, 2018.
[44] K. Satyanarayana, M. El-Hajjar, P.-H. Kuo, A. Mourad, and L. Hanzo, "Dual-function hybrid beamforming and transmit diversity aided millimeter wave architecture," *IEEE Trans. Veh. Technol.*, vol. 67, no. 3, pp. 2798–2803, Mar. 2018.
[45] C. Rusu, R. Mèndez-Rial, N. González-Prelcic, and R. W. Heath, Jr., "Low complexity hybrid precoding strategies for millimeter wave communication systems," *IEEE Trans. Wireless Commun.*, vol. 15, no. 12, pp. 8380–8393, Dec. 2016.
[46] X. Zhang, A. F. Molisch, and S.-Y. Kung, "Variable-phase-shift-based RF-baseband codesign for MIMO antenna selection," *IEEE Trans. Signal Process.*, vol. 53, no. 11, pp. 4091–4103, Oct. 2005.
[47] A. Ahmed, P. Botsinis, S. Won, L. L. Yang, and L. Hanzo, "Exit chart aided convergence analysis of recursive soft m-sequence estimation in Nakagami-m fading channels," *IEEE Trans. Veh. Technol.*, vol. 67, no. 5, pp. 4655–4660, Jan. 2018.
[48] A. Ahmed, P. Botsinis, S. Won, L.-L. Yang, and L. Hanzo, "Primitive polynomials for iterative recursive soft sequential acquisition of concatenated sequences," *IEEE Access*, vol. 7, pp. 13882–13900, 2019.
[49] S. Han, I. Chih-Lin, Z. Xu, and C. Rowell, "Large-scale antenna systems with hybrid analog and digital beamforming for millimeter wave 5G," *IEEE Commun. Mag.*, vol. 53, no. 1, pp. 186–194, Jan. 2015.
[50] J. G. Andrews, S. Buzzi, W. Choi, S. V. Hanly, A. Lozano, A. C. K. Soong, and C. J. Zhang, "What will 5G be?" *IEEE J. Sel. Areas Commun.*, vol. 32, no. 6, pp. 1065–1082, Jun. 2014.
[51] P. Wang, Y. Li, L. Song, and B. Vucetic, "Multi-gigabit millimeter wave wireless communications for 5G: From fixed access to cellular networks," *IEEE Commun. Mag.*, vol. 53, no. 1, pp. 168–178, Jan. 2015.
[52] D. Torrieri, S. Talarico, and M. C. Valenti, "Analysis of a frequency-hopping millimeter-wave cellular uplink," *IEEE Trans. Wireless Commun.*, vol. 15, no. 10, pp. 7089–7098, Aug. 2016.
[53] J. Song, J. Choi, and D. J. Love, "Codebook design for hybrid beamforming in millimeter wave systems," in *Proc. IEEE Int. Conf. Commun. (ICC)*, Jun. 2015, pp. 1298–1303.
[54] J. Song, J. Choi, and D. J. Love, "Common codebook millimeter wave beam design: Designing beams for both sounding and communication with uniform planar arrays," *IEEE Trans. Commun.*, vol. 65, no. 4, pp. 1859–1872, Apr. 2017.
[55] R. Rajashekar and L. Hanzo, "Hybrid beamforming in mm-Wave MIMO systems having a finite input alphabet," *IEEE Trans. Commun.*, vol. 64, no. 8, pp. 3337–3349, Jun. 2016.

[56] B. Clerckx, Y. Zhou, and S. Kim, "Practical codebook design for limited feedback spatial multiplexing," in *Proc. IEEE Int. Conf. Commun.*, May 2008, pp. 3982–3987.
[57] A. Ahmed, "Iterative initial synchronization in wireless communications," Ph.D. dissertation, Next Wireless Group ECS, Univ. Southampton, Southampton, U.K., Mar. 2019. [Online]. Available: https://eprints.soton.ac.uk/437692/
[58] Y. T. Su and L.-D. Jeng, "Antijam capability analysis of RS-coded slow frequency-hopped systems," *IEEE Trans. Commun.*, vol. 48, no. 2, pp. 270–281, Feb. 2000.
[59] Y. T. Su and R. C. Chang, "Performance of fast FH/MFSK signals in jammed binary channels," *IEEE Trans. Commun.*, vol. 42, no. 7, pp. 2414–2422, Jul. 1994.
[60] A. Ahmed, Z. Elsaraf, F. A. Khan, and Q. Z. Ahmed, "Cooperative non-orthogonal multiple access for beyond 5G networks," *IEEE Open J. Commun. Soc.*, vol. 2, pp. 990–999, 2021.
[61] A. Alkhateeb, G. Leus, and R. W. Heath, Jr., "Limited feedback hybrid precoding for multi-user millimeter wave systems," *IEEE Trans. Wireless Commun.*, vol. 14, no. 11, pp. 6481–6494, Nov. 2015.
[62] A. Klappenecker and M. Rötteler, "Constructions of mutually unbiased bases," in *Finite Fields and Applications*. Springer, 2004, pp. 137–144.
[63] T. Inoue and R. W. Heath, Jr., "Kerdock codes for limited feedback precoded MIMO systems," *IEEE Trans. Signal Process.*, vol. 57, no. 9, pp. 3711–3716, Sep. 2009.
[64] A. Ahmed, Q. Z. Ahmed, A. Rehman, and S. Karim, "The performance of fast frequency hopping system in additive white Gaussian noise (AWGN)," *Int. J. Comput. Appl.*, vol. 46, pp. 106–113, May 2012.
[65] L. Hanzo, H. Haas, S. Imre, D. O'Brien, M. Rupp, and L. Gyongyosi, "Wireless myths, realities, and futures: From 3G/4G to optical and quantum wireless," *Proc. IEEE*, vol. 100, no. Special Centennial Issue, pp. 1853–1888, May 2012.
[66] B. Friedlander and S. Scherzer, "Beamforming versus transmit diversity in the downlink of a cellular communications system," *IEEE Trans. Veh. Technol.*, vol. 53, no. 4, pp. 1023–1034, Jul. 2004.
[67] D. Torrieri and M. C. Valenti, "The outage probability of a finite ad hoc network in Nakagami fading," *IEEE Trans. Commun.*, vol. 60, no. 11, pp. 3509–3518, Aug. 2012.

ABBAS AHMED received the B.E.E. degree in electrical engineering (specialization in electronics) from Air University, Islamabad, Pakistan, in 2007, and the M.Sc. degree (Hons.) and the Ph.D. degree in electronics and electrical engineering from the University of Southampton, U.K., in 2009 and 2019, respectively. During his Ph.D. degree, he worked on synchronization issues for wireless communication system. He has designed diverse algorithms by using iterative decoding. He was working as a Research Fellow with the University of Leeds and a Research Assistant with the University of Huddersfield. He is currently working as a Programme Head with the Electrical and Electronics Engineering Department, Beaconhouse International College, Islamabad, affiliated with Liverpool John Moores University, U.K. His major research interests include initial synchronization, iterative detection, device to device communications, mm waves communication, cooperative communication, and fast frequency hopping systems.

QASIM ZEESHAN AHMED (Member, IEEE) received the degree in electrical engineering from the National University of Science and Technology, Pakistan, in 2001, the M.Sc. degree in electrical engineering from the University of Southern California (USC), Los Angeles, USA, in 2005, and the Ph.D. degree in electronics and electrical engineering from the University of Southampton, U.K., in 2009. During his Ph.D. degree, he worked on ultra-wide bandwidth systems. From 2009 to 2011, he was working as an Assistant Professor at the National University of Computer and Emerging Sciences (NUCES), Islamabad, Pakistan. In 2011, he started working as a Postdoctoral Fellow in cooperative communications at the King Abdullah University of Science and Technology (KAUST). In 2015, he started working as a Lecturer at the University of Kent, where he was involved with research on millimetre wave and device to device communications. He is currently a Lecturer in electronic and electrical engineering at the University of Huddersfield, U.K. His major research interests include wireless communications, millimeter wave communications, ultra wide bandwidth systems, device to device communications, and cooperative communication.

AHMAD ALMOGREN (Senior Member, IEEE) received the Ph.D. degree in computer science from Southern Methodist University, Dallas, TX, USA, in 2002. He is currently a Professor with the Computer Science Department, College of Computer and Information Sciences (CCIS), King Saud University (KSU), Riyadh, Saudi Arabia, where he is the Director of the Cyber Security Chair, CCIS. Previously, he worked as the Vice Dean of development and quality at CCIS. He also served as the Dean for the College of Computer and Information Sciences and the Head for the Academic Accreditation Council, Al Yamamah University. His research interests include mobile pervasive computing and cyber security. He served as a Technical Program Committee Member for numerous international conferences/workshops, such as IEEE CCNC, ACM BodyNets, and IEEE HPCC. He served as the General Chair for the IEEE Smart World Symposium.

SYED KAMRAN HAIDER received the B.S. degree in telecommunication engineering from Foundation University, Rawalpindi Campus, Pakistan, in 2015, and the M.S. degree in information and communication engineering from Hohai University (HHU), Changzhou Campus, China, in 2018, where he is currently pursuing the Ph.D. degree. Furthermore, he is working as a Lecturer with the Electrical and Electronics Engineering Department, Beaconhouse International College (BIC), Islamabad, Pakistan, affiliated with Liverpool John Moores University, U.K. His research contributed in the domain of EEG signal classification, signal processing, mm wave communication, wireless sensor networks (WSNs) optimization, and UAV flight path modeling.

ATEEQ UR REHMAN was born in Rawalpindi, Pakistan, in 1987. He received the B.S. degree in electrical (telecommunication) engineering from the COMSATS Institute of Information Technology, Lahore, Pakistan, in 2009, and the M.S. degree in electrical engineering with a specialization in telecommunications from the Blekinge Institute of Technology (BTH), Karlskrona, Sweden, in 2011. He is currently pursuing the Ph.D. degree with the College of Internet of Things (IoT) Engineering, Hohai University (HHU), Changzhou Campus, China. From 2011 to 2012, he was a Lecturer with the Department of Electrical Engineering, University of South Asia, Lahore. From 2012 to 2016, he joined the Faculty of Engineering and Technology, The Superior College (University Campus), Lahore, in the capacity of a Lecturer. Since 2016, he has been working as a Lecturer at Government College University (GCU), Lahore. He has contributed to various international IEEE conferences and journals of repute. His research interests include biomedical signal processing, the Internet of Things (IoTs), Social Internet of Things (SIoTs), big data, and renewable energy technologies.